Prediction of the force of the ball-burnishing, physical model

Hernán A. González Rojas (1), José A. Travieso Rodríguez (2)

(1) Departamento de Ingeniería Mecánica - Universidad Politécnica de Cataluña, Av. Diagonal 647, 08028 Barcelona, Spain, hernan.gonzalez@upc.edu
(2) Departamento de Ingeniería Mecánica - Universidad Politécnica de Cataluña, C/ Comte d'Urgell 187, 08036 Barcelona, Spain, antonio.travieso@upc.edu

RESUMEN

En este artículo se desarrolla un modelo físico para predecir la fuerza en el bruñido con bola. El modelo está construido en base a la teoría de la plasticidad. En el desarrollo del modelo se ha encontrado el número adimesional *B* que caracteriza el problema de deformación plástica en el bruñido con bola. Los experimentos realizados en acero y aluminio permiten validar el modelo y destacar la correcta predicción de las tendencias de comportamiento del bruñido con bola.

Palabras clave: Bruñido con bola; Manufactura de superficie; Deformación plástica

ABSTRACT

In this paper, we have developed a physical model to predict the forces of the ball burnishing. The models have been constructed on the basis of the plasticity theory. During the model development we have figured out the dimensionless number *B* that characterizes the problem of plastic deformation in the ball-burnishing. The experiments performed in steel and aluminum allow to validate the model and to emphasize the correct prediction of behaviour patterns that the model describe.

Keywords: Ball-burnishing; Surface manufacturing; Plastic deformation

1. Introducción

Ball-burnishing is a surface finishing process that consists in making a ball roll, which deforms the material surface by applying a compression force. In general this is a process of low energetic cost as it is a cold-working process, which can be applied by the same machine that has mechanized the work-piece before. Thus the process is interesting from the point of view of manufacturing industry [1]. On the one hand ball-burnishing is used among other reasons to improve the superficial roughness of plastic injection mould surfaces [2]. On the other hand, the compression tensions induced on the material surface increases the superficial resistance of the work-pieces [3]. An increased superficial resistance of the material produces a rising fatigue resistance. Therefore the material carries dynamic loads better [4]. In general the burnishing process changes the maximum residual stress from the traction to compression. This generates an increase the burnishing stresses [5] or which is the same; this produces a hardening by deformation of the material surface. The plastic flow of the first material layer occurs when maximum tension condition exceeds the yield stress [6]. On the other hand, Gao *et al.* [7] developed models for describing indentation deformations of elastic strain-hardening materials. They show that for a given indenter geometry, indentation hardness depends on: Young's modulus, yield stress and strain-hardening index of the indented material.

In various papers the Experimental Design (DOE) is commonly used to determine the influence and importance of the different variables involved in the burnishing process. In general, the influences of burnishing conditions and material properties on superficial roughness and micro-hardness have been analysed. The most common technologies are: Response Surface Methodology (RSM) [5] and Factorial Design [3]. In El-Axir [5] he reported the results of an experimental program to study the influence of different burnishing conditions on surface micro-hardness and roughness. He studied the four variables: burnishing speed, force, feed, and number of passes. Also, he reported the relation between residual stress and burnishing. Mathematical models are presented for predicting the surface micro-hardness and roughness of St-37, caused by roller burnishing under lubricated conditions. Luca et al [3], studied the surface finish on heat-treated steel, using a factorial experiment. They analyzed the influence of variables such as: burnishing feed, hard turning feed and normal burnishing force, in the surface roughness. They mentioned that the burnishing obtained is very similar to those one obtained by grinding.

The same method was applied to other experiments studying surface roughness and material hardening in burnishing with ball or roll. Shiou and Chen [2] studied four burnishing parameters: the ball material, burnishing speed, burnishing force, and feed. They were selected as the experimental factors of Taguchi's design of experiment to determine the optimal burnishing parameters, which have the dominant influence on surface roughness. Hassan [1] performed an experimental study of roller burnishing tools. The performance of the tools, plus the burnishing force effects, the number of burnishing tool passes on the surface roughness, surface hardness of commercially available aluminium and brass were studied. Hamadache et al. [8] developed a device for mechanical plastic deformation of structural Rb40 steel using ball and roller burnishing. They investigated the evolution of the association between roughness, hardness and wear resistance. They found that roller burnishing provides optimal roughness results, particularly when initial surface quality is close to 3µm whereas in terms of hardness, ball burnishing becomes interesting.

In this paper we present the development and validation of a physical model to predict the forces in the burnishing process. This model has been developed from a force balance equation applied to a free body with differential thickness.

2. Physical Model

The approximation to predict the forces in the burnishing process corresponds to a model obtained from a force balance equation applied to a differential element, see figure 1a. The hypotheses used to construct this first model are:

- The ball of burnishing is considered a rigid body and the burnished material is considered a perfect plastic material.
- The plastic flow corresponds to an issue of plane stress.
- There is no friction between the ball and the material.
- The material surface is continuous, neither valleys nor superficial peaks exist.

The model shows the burnishing force *F* as a function of the ball diameter *D*, the burnishing depth *e* and the yield limits for pure tension *Y0*.

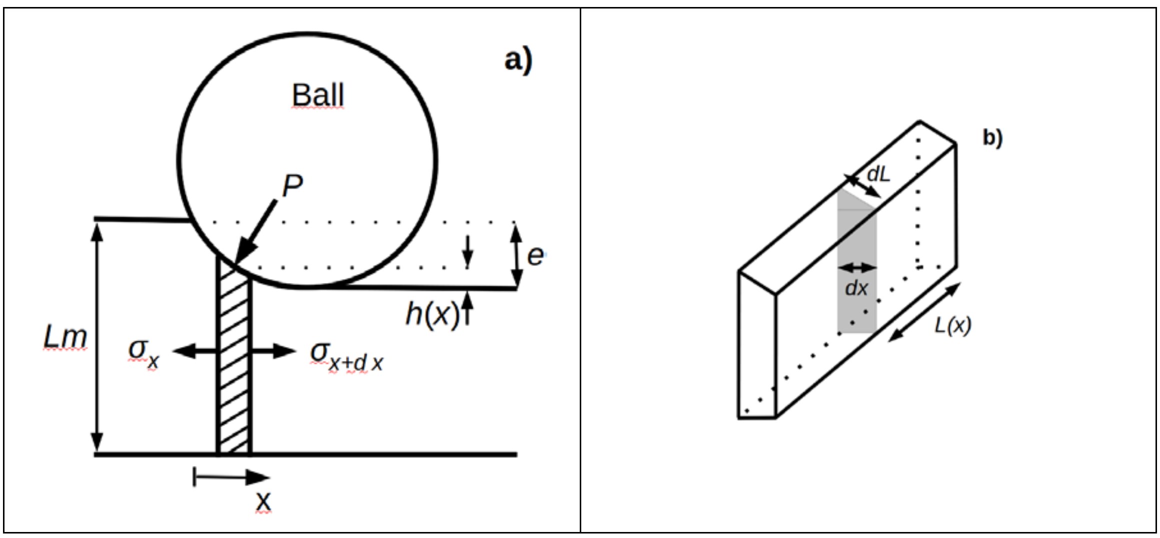

Figure 1. *Ball-burnishing process. a) Zone of plastic deformation, b) Differential element*

After doing a forces balance on a one-dimensional infinitesimal element, see figure 1b, a differential ordinary equation was obtained with following variables: the traction stress in horizontal direction σ and the burnishing pressure *P*. Both are a function of the position *x*.

$$\frac{d(\sigma\, A)}{dx} + P\, L(x)\frac{dh(x)}{dx} = 0 \tag{1}$$

Where *A* is a normal section to the tension *σ*, defined as: the height of the material (*Lm*-*e*) multiplied by the contact length of the ball-material *L(x)*, see figure. 1b. In general, *Lm* is larger than *e*, therefore *A* is defined as:

$$A = Lm\, L(x) \tag{2}$$

The contact length of the ball-material *L*(*x*) is defined depending on the depth of burnishing *e*, and the height *h*(*x*), see figure 1a.

$$L(x) = \sqrt{D\left(e - h(x)\right)} \tag{3}$$

With *h*(*x*) defined as

$$h(x) = \frac{\left(\sqrt{D\,e} - x\right)^2}{D} \tag{4}$$

The dimensionless equations are obtained replacing the following linear-transformations in (1-4)

$$x^* = \frac{x}{\sqrt{D\,e}} \qquad \sigma^* = \frac{\sigma}{Y_0} \qquad P^* = \frac{P}{Y_0} \tag{5}$$

Replacing the equations (2, 3, 4 and 5) in the differential equation (1), the equation of dimensionless linear momentum, associated to the problem of burnishing with a ball is obtained.

$$\frac{d\sigma^*}{dx^*} + (1 - x^*) \quad \frac{\sigma^*}{\left(2x^* - x^{*2}\right)} \quad P^* 2\frac{e}{Lm} \quad = 0 \tag{6}$$

The first model the tension problem of burnishing is treated as a deformation problem of a perfect plastic. The plastic behavior of the material is introduced by means of the von Mises yield criterion [9] that in the dimensionless form is as follows

$$\sigma^* + P^* = \frac{2}{\sqrt{3}} \tag{7}$$

Therefore, the stress field must fulfill the criterion of plasticity (7). Replacing (7) in (6) the following equation is obtained

$$\frac{d\sigma^*}{dx^*} + (1 - x^*)\sigma^* \quad \frac{1}{2x^* - x^{*2}} + 2\frac{e}{Lm} \quad = (1 - x^*)2\frac{2}{\sqrt{3}}\frac{e}{Lm} \tag{8}$$

In this equation, σ* is the only function of the space x*, with a domain defined between [0, 1]. Finally, the model is completed if the initial condition of the problem is defined as:

$$\sigma^*\big|_{x^*=0} = 0 \tag{9}$$

The developed model it is statically determinated. The equation solution (8) with the initial condition (9) allows to find the stress distribution in the material under the burnishing ball.

The equation (8) is solved by the Finite Differences Method. Once the stress distribution σ^*_i, regarding a discreet domain has been obtained, the distribution of discreet pressure P^*_i, through the equation (7) is achieved.

The dimensionless pressure is constant and equal to $\frac{2}{\sqrt{3}}$, for any value within this interval:

$$0{,}00002 \leq \frac{e}{Lm} \leq 0{,}001 \tag{10}$$

Once the pressure *P** has been determined, it is possible to estimate the force of burnishing in vertical direction (*F*). Therefore the pressure function is integrated into the top area showed in the Figure 1b.

$$F = \int_0^L P(x)\, 2\, L(x) dx \tag{11}$$

By dividing the equation (11) by the yield limit for pure tension and by introducing the equations (5) the dimensionless burnishing force *F** is obtained:

$$F^* = \int_0^1 P^*(x^*) D\, e\, 2\sqrt{\left(2x^* - x^{*2}\right)} dx^* \tag{12}$$

The vertical dimensionless force of burnishing is obtained by integrating (12).

$$F^* = P^* D\, e \frac{\pi}{2} \tag{13}$$

From the equation (13) number *B* is defined, which characterizes the problem of burnishing.

$$B = \frac{F}{Y_0\, D\, e} \tag{14}$$

For this model the number *B* is constant and equal to $\frac{\pi}{\sqrt{3}}$, if *P** is equal to $\frac{2}{\sqrt{3}}$.

3. Validation

Two different materials have been simulated: aluminium A96351 and steel G10380. The properties of these materials have been experimentally determined and summarized in the Table I. The burnishing conditions are summarized in Table II.

Table I. Materials properties

	K	*n*	Y_0
A96351	368MPa	0.26	140MPa
G10380	1117MPa	0.19	416MPa

Table II. Experiment conditions

Ball Diameter *D*	10mm
Height of the material *Lm*	30mm
Burnishing speed	200mm/min

Two processes of burnishing in two different materials were done to validate the models. A spherical milling tool of 4mm of diameter and two edges was used in the previously mechanized of the work-pieces. The cutting conditions were: rotational velocity of the tool 12000min^{-1}, feed speed 16.6mm/s, cutting depth 0.5mm and the lateral-steep 0.5mm. The aluminium used in the experiments is shown in Figure 2, where the vertical bands correspond to the burnished surface. The feed speed of the ball is perpendicular to the feed per tooth of the milling in all the experiments.

Figure. 2. *Work-piece of burnished aluminium*

The validation consists on determine the *B* number for the experiments. In Tables I and II the material properties and the cutting conditions are respectively summarized. In Table I the yield stress Y_0 for both materials is shown. In Table II the diameter of the ball *D* and the height of the work-piece *Lm* are shown. Therefore, to evaluate the *B* number is necessary to know the burnishing depth *e* and the force *F* for the different experiments. For determination of the burnishing depth is necessary done measuring the jump between the burnished area topography (Zone 2) and the milling area topography (Zone 1) in each experiments. The jump is determined from a superficial roughness chart, see Figure 3. In the Zone 1 we can see the fingerprints left by the successive passage of the milling tool, and in the Zone 2 it is possible to see the burnished surface. In this case, the burnishing depth is equal to 4.6μm and it is defines as the difference of height between both surfaces. Finally, the force *F* is measured on a dynamometer table manufactured by Kistler.

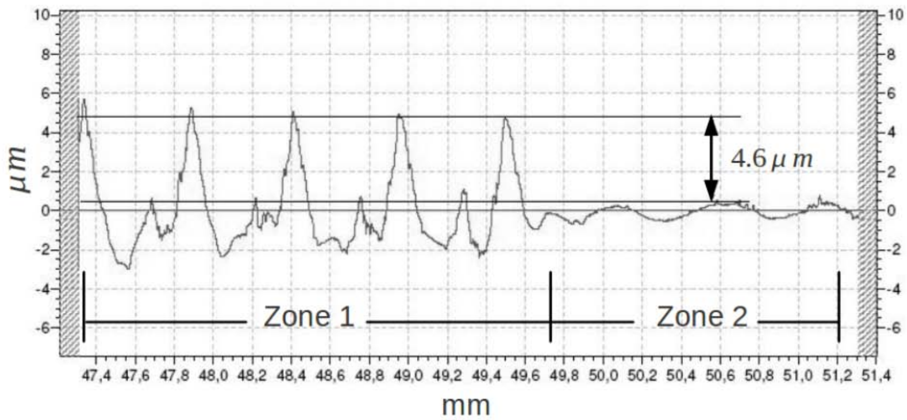

Fig. 3. *Milled and burnished surface topography*

Six different experiments were made. Three burnishing processes were done in steel and other three in aluminium. The cutting conditions of the milling tool are the same for both materials; therefore the superficial topography produced by the milling machine is the same in all the experiments. The topography of the burnished surfaces is different because they were done applying different burnishing forces. The Figure 4 shows simultaneously the results of the six experiments and the simulation done with the model.

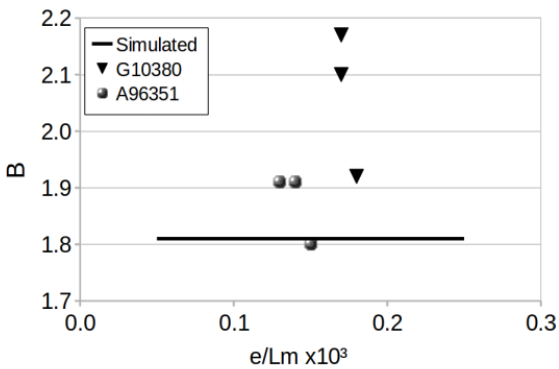

Figure. 4. *Number B simulated v/s experiments*

In this figure it is possible to see how the model reproduces correctly the behaviour in the burnishing process. The number *B* obtained in the three experiments done with aluminium, it is closer to the number *B* obtained theoretically, the error in the prediction of B is less than 5%.
In contrast, the number *B* obtained in the three experiments done with steel, is farther from the theoretical *B* number, the average error in the prediction is 15%. This is likely due to the burnishing speed (*Va*=200m/min), which produces hardening in the steel. In contrast in aluminium, hardening does not occur at this speed burnishing.

4. Conclusiones

A physical model has been developed to predict the burnishing forces. It is based on the Theory of Plasticity.

The problem of the stresses in the ball-burnishing process is characterized by the *B* dimensionless number.

5. Acknowledgements

The authors of this paper would like to thank Dr. Gilles DESSEIN from the ENIT LGV, for his cooperation for conducting experiments concerning this article.

6. Referencias

[1] A.M. Hassan, *The effects of ball- and roller-burnishing on the surface roughness and hardness of some non-ferrous metals*, J. Mater. Process. Technol. 72 (1997) 385-391.

[2] F-J. Shiou and CH. Chen, *Freeform surface finish of plastic injection mold by using ball-burnishing process*, J. Mater. Process. Technol. 140 (2003) 248-254.

[3] L. Luca, S. Neagu-Ventzel and, I. Marinescu, *Effects of working parameters on surface finish in ball-burnishing of hardened steels*, Prec. Eng. 29 (2005) 253-256.

[4] F. Klocke and J. Liermann, *Roller burnishing of hard turned surface*, Int. J. Mach. Tools. Manuf. 38 (1998) 419-423.

[5] M.H. El-Axir, *An investigation into roller burnishing*, Int. J. Mach. Tools. Manuf. 40 (2000) 1603-1617.

[6] R.L. Murthy and B. Kotiveerachari, *Burnishing of hard turned surface*, Prec. Eng. 3 (1981) 172-179.

[7] X-L. Gao, X.N. Jing and G. Subhash, *Two new expanding cavity models for indentation deformations of elastic strain-hardening materials*, Int. J. Solids. Struct. 43 (2007) 2193-2208.

[8] H. Hamadache, L, Laouar, N.E. Zeghib and K. Chaoui, *Characteristics of Rb40 steel superficial layer under ball and roller burnishing*, J. Mater. Process. Technol. 180 (2006) 130-136.

[9] J. Chakrabarty, *Theory of Plasticity*, Elsevier 3ªEd., Oxford (UK), 2006.